Available online at www.sciencedirect.com
ScienceDirect
ELSEVIER
February 2011, 18(1): 28–35
www.sciencedirect.com/science/journal/10058885
The Journal of China Universities of Posts and Telecommunications
http://www.jcupt.com

Layered space time codes and capacity analysis in correlated fading channels with distributed antenna system

XIONG Fei (✉), ZHANG Jian-hua, ZHANG Ping

Wireless Technology Innovation Institute, Key Laboratory of Universal Wireless Communication, Ministry of Education, Beijing University of Posts and Telecommunications, Beijing 100876, China

Abstract

In this paper we have investigated the performance of downlink generalized distributed antenna system (GDAS). Under the assumption of spatial correlated fading conditions, we have derived the numeric expression of correlated coefficients according to series of Bessel function, and have lifted the range restriction of the mean angle of incident. Moreover, the architecture of distributed generalized layered space time codes (GLST) has been considered in order to achieve both multiplexing gain and diversity gain while we have used basis vector from null space instead of orthogonal set to obtain the same system performance but with lower complexity. Furthermore, in order to maximize the capacity, Gerschgorin circles based fast antenna selection algorithms have been evaluated including a discussion of those simulation results.

Keywords GDAS, GLST, capacity, correlated fading channel

1 Introduction

In the next generation mobile communications, GDAS has attracted wide research interests in recent years, because it provides an effective way to extend the coverage areas and lower the demands of transmitter power [1–2], thus it can well meets the requirement for the design of future wireless networks.

From the perspective of previous studies, vertical bell labs layered space time (VBLAST) and space time block code (STBC) have been considered as two extreme methods to achieve multiplexing and diversity gain separately in multiple-input multiple-output (MIMO) system [3–4]. In this study, the architecture of distributed GLST has been proposed in order to achieve both multiplexing and diversity gain simultaneously. Moreover, in the real propagation conditions, the fading channels are not independent but spatial correlated between the transmission links [5]. Therefore, we deduced the correlation coefficients between two antenna elements as a function of the power angular spread (PAS), antenna spacing, angle of departure (AoD) and azimuth spread (AS). Furthermore in Refs. [6–7], Norm and Gram-Schmidt based antenna selection algorithms have been proposed, but without considering the effects of correlated fading channels, thus, we utilize the Gerschgorin circles theory to solve the problems.

Motivated by previous work, in this study we analyze the downlink cellular GDAS performance under spatial correlated fading channels, from which the correlation coefficients have been derived from series of Bessel function. Different from [8], here we have lifted the restriction with the mean angle of incident and shared a common method in deducing the correlation coefficients. Moreover, in multiplexing technology [9], the decoding algorithms require that the receiver antenna numbers should be greater than or at least equal with the transmit antenna numbers; otherwise, it will results in poor performance. However it is not practical when mobile terminal has less receive antennas than transmitter, thus, in this paper we utilize the basis vectors in nulling space to solve the problems. Furthermore by using Gerschgorin circles based fast antenna selection algorithms we can increase the system capacity even in more sever correlated conditions.

The remainder of this paper is organized as follows. Sect. 2

Received date: 03-06-2010
Corresponding author: XIONG Fei, E-mail: xiongfei@mail.wtilabs.cn
DOI: 10.1016/S1005-8885(10)60024-6

describes the system structures and spatial correlated fading channel models. Sect. 3 gives the encoder structure and decoding algorithms for the distributed generalized layered space time codes in GDAS, and presents the system performance in the correlated fading conditions. Sect. 4 shows the fast antenna selection algorithms based on the Gerschgorin circles theory, including a discussion of those simulation results in terms of system capacity. Finally, Sect. 5 draws a brief conclusion of the subjects discussed in the previous sections.

2 System description and channel model

2.1 System description

In this study we mainly concern about the downlink flat-fading general distributed antenna system GDAS (*M*, *N*, *L*), which employs *N* ports, *L* antennas per port and *M* antennas for each mobile terminal. The system architecture has shown in Fig. 1.

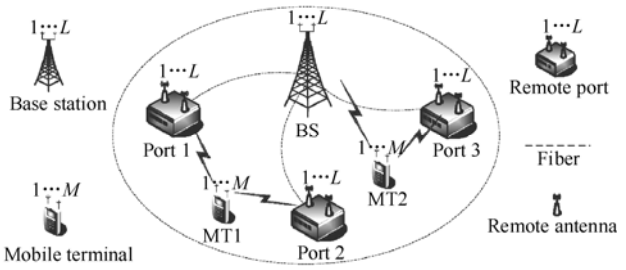

Fig. 1 The architecture of generalized distributed antenna system

Here we denote base station (BS) as a central port; hence, the received signals at mobile terminal (MT) could be expressed as

$$\boldsymbol{y}=\sqrt{P}\boldsymbol{H}\boldsymbol{x}+\boldsymbol{z} \tag{1}$$

where $\boldsymbol{x}$ represents transmit signals with $\boldsymbol{E}[|\boldsymbol{x}|^2]=1$ (Note: $\boldsymbol{E}[.]$ is expectation operator), $\sqrt{P}$ is signal power from *k*th port to MT, symbol z is independent identical distribution (i.i.d) complex additive white Gaussian noise (AWGN) with variance σ_z^2. Then the channel matrix $\boldsymbol{H}$ can be expressed as

$$\boldsymbol{H}=\left[\boldsymbol{H}^{(1)}(d_1),\boldsymbol{H}^{(2)}(d_2),...,\boldsymbol{H}^{(k)}(d_k),...,\boldsymbol{H}^{(N)}(d_N)\right] \tag{2}$$

where $\boldsymbol{H}^{(k)}(d_k)$ is a function of distance d_k with dimension of $M\times L$ matrix and the superscript *k* stands for *k*th port $(k=1,2,...,N)$, and $h_{i,j}^{(k)}(i=1,2,...,M;j=1,2,...,L)$ is the entry of $\boldsymbol{H}^{(k)}(d_k)$ from *j*th antenna element in *k*th port to the *i*th receiver, which including small scale fading, path loss and shadow fading. Here, the small scale fading is modeled as zero-mean complex Gaussian random variable with variance s_n, and the mean of s_n is equal to path loss at the given port, which is modeled as lognormal random variable.

2.2 Correlated channel model

It is assumed that the channel variation is negligible over several symbol periods, comprising a packet of symbols. Moreover, the channel is estimated accurately, thus, for brevity in the rest of the paper, we will make no distinction between $\boldsymbol{H}$ and its estimate. However, when considering the downlink semi-correlated fading conditions, the channel model in Eq. (1) can be rewritten as:

$$\boldsymbol{H}=\boldsymbol{H}_w\boldsymbol{L}_{\mathrm{Tx}} \tag{3}$$

where $\boldsymbol{L}_{\mathrm{Tx}}$ is $n_{\mathrm{Tx}}\times n_{\mathrm{Tx}}$ lower transmit triangular matrices with positive diagonal elements and n_{Tx} denotes transmit antenna numbers. It can be derived from positive definite correlation matrices $\Omega=\boldsymbol{L}_{\mathrm{Tx}}\boldsymbol{L}_{\mathrm{Tx}}^{\mathrm{H}}$ (Note: $(.)^{\mathrm{H}}$ is Hermitian operator) by Cholesky decomposition, and $\boldsymbol{H}_w$ is the channel matrix with uncorrelated complex Gaussian entries. According to Ref. [8], we can further deduce the expressions of cross correlation coefficients as

$$\left.\begin{aligned}\Omega_{x,x}&=\int_{\theta-\Delta}^{\theta+\Delta}\cos\left(2\pi\frac{d_{n_1,n_2}}{\lambda}\sin\ \Phi\right)f(\Phi)\mathrm{d}\Phi\\ \Omega_{x,y}&=\int_{\theta-\Delta}^{\theta+\Delta}\sin\left(2\pi\frac{d_{n_1,n_2}}{\lambda}\sin\ \Phi\right)f(\Phi)\mathrm{d}\Phi\end{aligned}\right\} \tag{4}$$

where $\Omega_{x,x}$ is the correlation coefficient between the real parts of $h_{x_1,y}^{(k)}$ and $h_{x_2,y}^{(k)}$, and $\Omega_{x,y}$ is the correlation coefficient between the real parts of $h_{x_1,y}^{(k)}$ and the imaginary parts of $h_{x_2,y}^{(k)}$. Here λ is the wavelength, d_{n_1,n_2} is the distance between the transmit antenna elements n_1 and n_2, and we use normalized distance z to represent $2\pi d_{n_1,n_2}/\lambda$ in the following part. While θ is the plane-wave AoD, and Δ is the angular spread (AS). Different from Ref. [8], here we have lifted mean incident angle restrictions by introducing a parameter Δ such that the PAS is defined over $[\theta-\Delta<\Phi<\theta+\Delta]$. By making use of the series representations of Bessel function [See Ref. [10] p.145] we can obtain

$$\left.\begin{aligned}\cos(z\sin\Phi)&=J_0(z)+2\sum_{m=1}^{\infty}J_{2m}(z)\cos(2m\Phi)\\ \sin(z\sin\Phi)&=2\sum_{m=0}^{\infty}J_{2m+1}(z)\sin[(2m+1)\Phi]\end{aligned}\right\} \tag{5}$$

where $J_r(z)$ is rth order Bessel function of first class. It has been shown in Ref. [11] that Laplacian PAS is closer in fitting with measured data at transmitter, and the probability density function (pdf) of Laplacian distribution [11] can be given as

$$f(\Phi)=N_0\exp\left(\frac{-\sqrt{2}\,|\Phi-\theta|}{\sigma}\right)G(\Phi) \tag{6}$$

where θ is AoD, σ is the RMS angular spread and both angles Φ and θ are given with respect to the bore sight of the antenna elements. For simplicity, here we assume the base station antenna gain $G(\Phi)$ equals to $\left(\sqrt{2}\sigma\right)^{-1}$, and N_0 is a normalized constant that satisfied with

$$\int_{-\pi}^{\pi}f(\Phi)\mathrm{d}\Phi=\int_{\theta-\Delta}^{\theta+\Delta}N_0\exp\left(\frac{-\sqrt{2}\,|\Phi-\theta|}{\sigma}\right)G(\Phi)\mathrm{d}\Phi=1 \tag{7}$$

which leads to

$$N_0=\left[1-\exp\left(-\frac{\sqrt{2}\Delta}{\sigma}\right)\right]^{-1} \tag{8}$$

Then we substitute Eqs. (5)–(8) into Eq. (4), and the correlation coefficients of Laplacian PAS can be expressed as (See Appendix A and B)

$$\Omega_{x,x}=J_0(z)+2\tau N_0\sum_{\xi=2m>0}\frac{J_\xi(z)\cos(\xi\theta)}{[(\xi)^2+(\tau)^2]}\cdot [\tau+e^{-\pi\Delta}(\xi\sin(\xi\Delta)-\tau\cos(\xi\Delta))] \tag{9}$$

and

$$\Omega_{x,y}=2\tau N_0\sum_{\upsilon=2m+1>0}\frac{J_\upsilon(z)\sin(\upsilon\theta)}{[(\upsilon)^2+(\tau)^2]}\cdot [\tau+\mathrm{e}^{-\pi\Delta}(\upsilon\sin(\upsilon\Delta)-\tau\cos(\upsilon\Delta))] \tag{10}$$

where $\xi=[2,4,...,\infty],\upsilon=[1,3,...,\infty]$ and $\tau=\sqrt{2}/\sigma$ separately. Thus, the envelope correlation Ω is defined as

$$\Omega=\sqrt{(\Omega_{x,x})^2+(\Omega_{x,y})^2} \tag{11}$$

3 GLST architecture and multiple stream transmission

In Sect. 2 we have deduced the correlation matrix according to series of Bessel function. In Sect. 3, we further consider multi-stream transmission schemes combined with STBC and BLAST techniques in the semi-correlated MIMO channels.

3.1 Architecture of distributed GLST system

In this part we will propose distributed GLST architecture combined with BLAST and STBC under the spatial correlated fading conditions, although little attention has been paid nowadays to combine two techniques together in distributed antenna system. Here, STBC encoders are employed for each distributed antenna group to achieve the diversity gain, while multiple streams are transmitted from different groups simultaneously in order to obtain high spectral efficiency. To make it clear, the system architecture of transmitter has been shown in Fig. 2, where the distributed antennas are partitioned into q groups $G_1,G_2,...,G_q$, respectively, comprising n_1, $n_2,...,n_q$ antennas with $\sum_{i=1,2,...,q}n_i=n_{\mathrm{Tx}}$.

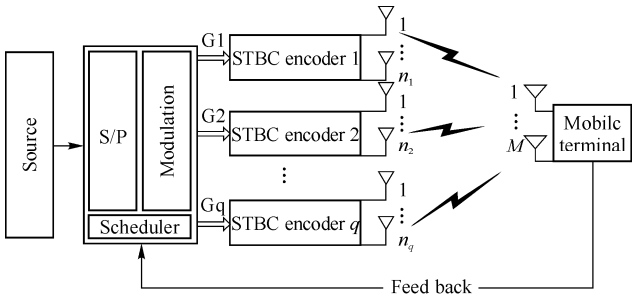

Fig. 2 The architecture of distributed GLST system

At transmitter side, the input information block B decomposes into the different groups as $B_1+B_2+...+B_q=B$. Through series to parallel transform each block B_i is then modulated to the M-order constellation symbols and encoded by a space-time block encoder to be x_i. At receiver side, GLST has a similar serial decoding structure as VBLAST, except all the interference nulling and interference cancellation are group based. To describe the group based interference suppression method, without loss of generality, we assume the previous $i-1$ groups have already been decoded and cancelled out from the received signals $\boldsymbol{y}_i^t,(t=1,2,...,T)$, and we should decode group i from the existed $i+1,i+2,...,q$ group inference signals. Here we assume the receiver knows the channel state information (CSI) and the not-yet-decoded groups $i+1,i+2,...,q$, can now be written as

$$\boldsymbol{y}_i^t=\boldsymbol{H}_i^t\boldsymbol{x}_i^t+\boldsymbol{H}_{i+1}^t\boldsymbol{x}_{i+1}^t+...+\boldsymbol{H}_q^t\boldsymbol{x}_q^t+\boldsymbol{z}_i^t \tag{12}$$

where $\boldsymbol{H}_i^t$ is $M\times n_i$ channel matrix, and $\boldsymbol{x}_i^t$ is $n_i\times 1$ transmit signals. Here, for simplicity we denote $V=n_{i+1}+n_{i+2}+...+n_q$ and $\boldsymbol{\eta}=[x_{i+1}^t,x_{i+2}^t,...,x_q^t]_{V\times 1}^{\mathrm{T}}$, $\boldsymbol{\Theta}=[H_{i+1}^t,H_{i+2}^t,...,H_q^t]_{M\times V}$, then Eq. (12) can be rewritten as

$$\boldsymbol{y}_i^t=\boldsymbol{H}_i^t\boldsymbol{x}_i^t+\boldsymbol{\Theta}\boldsymbol{\eta}+\boldsymbol{z}_i^t \tag{13}$$

where we assume the receive antenna $M\geqslant V+1$ and column rank $\boldsymbol{\Theta}=U\leqslant V$. In order to suppress the interference from the $i+1,i+2,...,q$ groups, we should find a set of basis vectors to constitute null space $N(\boldsymbol{\Theta})$,

which satisfied with

$$N(\boldsymbol{\Theta}) + \text{rank}\,\boldsymbol{\Theta} = M \tag{14}$$

Theorem 1 Assume $\boldsymbol{V}^m$ is sub-space of linear space $\boldsymbol{V}^n$ (n>m) in number field N, and $\boldsymbol{x}_1, \boldsymbol{x}_2, ..., \boldsymbol{x}_m$ is the basis of $\boldsymbol{V}^m$ with dimension m, then the existed basis $\boldsymbol{x}_1, \boldsymbol{x}_2, ..., \boldsymbol{x}_m$ could be extended to dimension n in $\boldsymbol{V}^n$ with a set of $n-m$ basis vectors $\boldsymbol{x}_{m+1}, \boldsymbol{x}_{m+2}, ..., \boldsymbol{x}_n$.

According to Theorem 1 [12], we can obtain $(M-U)\times M$ nulling matrix $\boldsymbol{\Lambda}$ such that $\boldsymbol{\Lambda}\times\boldsymbol{\Theta} = \{\boldsymbol{0}\}_{(M-U),V}$. Different from Ref. [3], $\boldsymbol{\Lambda}$ is not necessary to keep orthogonal because the nulling vector can be derived from solution space without requiring basis vectors to keep orthogonal to each other. In such way, we can obtain the same system performance with Ref. [3], but have lower implementation complexity. Then, multiply both sides of Eq. (13) by $\boldsymbol{\Lambda}$ we can obtain

$$\tilde{\boldsymbol{y}}_i^t = \tilde{\boldsymbol{H}}_i^t \boldsymbol{x}_i^t + \tilde{\boldsymbol{z}}_i^t \tilde{\boldsymbol{y}}_i^t \tag{15}$$

where $\tilde{\boldsymbol{y}}_i^t = \boldsymbol{\Lambda}\boldsymbol{y}_i^t$, $\tilde{\boldsymbol{H}}_i^t = \boldsymbol{\Lambda}\boldsymbol{H}_i^t$ and the equivalent noise vector $\tilde{\boldsymbol{z}}_i^t = \boldsymbol{\Lambda}\boldsymbol{z}_i^t$ is i.i.d complex Gaussian random variables with zero mean and $N_0/2$ variations. By using maximum likelihood space-decoder, we can decode the transmit signal as

$$\hat{\boldsymbol{x}}_i^t = \arg\min_x \sum_{t=1}^{T} |\, \tilde{\boldsymbol{y}}_i^t - \tilde{\boldsymbol{H}}_i^t \boldsymbol{x}_i^t \,|^2 \tag{16}$$

Thereafter we subtract the effect of the decoded group I from $\boldsymbol{y}_i^t$ before going to the next decoding level and we can obtain

$$\boldsymbol{y}_{i+1}^t = \boldsymbol{y}_i^t - \boldsymbol{H}_i^t \hat{\boldsymbol{x}}_i^t \tag{17}$$

Repeat the procedure Eqs. (12)–(17) until all groups are decoded correctly. Thus, by using the basis vector decoding algorithms, the requirement of receive antenna numbers have been relaxed to $M \geqslant \max\sum_{l=2}^{q} n_l' + 1$, and n_l' can be any set of the transmit antenna group $(n_1, n_2, ..., n_q)$, which makes it more suitable for the implementation of distributed MIMO system.

3.2 The simulation results for distributed GLST system

To illustrate the performance of distributed GLST system in the correlated fading channels, we consider a GDAS (M, N, L) MIMO system deploying uniform linear arrays (ULA) with 0.5-wavelength spacing between their elements at both ends. In the following part two different transmission schemes, namely GLST Co-MIMO (Collocated MIMO $N=1$) and GLST D-MIMO (Distributed MIMO $N\geqslant 2$) have been taken into considerations. In order to obtain the same diversity order $\tau = NLM$, we set M=4, N=1, L=4 for Co-MIMO and M=4, N=2, L=2 for D-MIMO respectively. Assuming the distance to each port is equal, thus we only consider the correlation between the adjacent antenna elements in each port, and ignore the effects of large scale fading. Without loss of generality we assume the AoD is zero degree and AS changes from 90°, 40° to 20°. Meanwhile 16 QAM modulations are used in the following part.

Let us consider the correlated channel model of GLST D-MIMO transmission. Since the distributed ports are sufficiently separated from each other, thus the correlation matrix is mainly dominated by adjacent antenna elements within each port. Therefore we can model the correlation matrix as follows

$$\boldsymbol{\Omega}_{\text{Tx},j} = \begin{bmatrix} \boldsymbol{1} & \boldsymbol{\Omega}_z^{(1,2)} & \cdots & \boldsymbol{\Omega}_z^{(1,L)} \\ \boldsymbol{\Omega}_z^{(2,1)} & \boldsymbol{1} & \cdots & \boldsymbol{\Omega}_z^{(2,L)} \\ \vdots & \vdots & & \vdots \\ \boldsymbol{\Omega}_z^{(L,1)} & \boldsymbol{\Omega}_z^{(L,2)} & \cdots & \boldsymbol{1} \end{bmatrix}_{L\times L} \tag{18}$$

where $\Omega_{\text{Tx},j}$ is the correlation matrix of port j($j = 1, 2, ..., N$) and $L = 2$, then the combined correlation matrix with N ports can be denoted as

$$\boldsymbol{\Omega}_{\text{Tx}} = \begin{bmatrix} \boldsymbol{\Omega}_{\text{Tx},1} & \boldsymbol{0}_{\boldsymbol{L}\times\boldsymbol{L}} & \cdots & \boldsymbol{0}_{\boldsymbol{L}\times\boldsymbol{L}} \\ \boldsymbol{0}_{\boldsymbol{L}\times\boldsymbol{L}} & \boldsymbol{\Omega}_{\text{Tx},2} & \cdots & \boldsymbol{0}_{\boldsymbol{L}\times\boldsymbol{L}} \\ \cdots & \cdots & & \cdots \\ \boldsymbol{0}_{\boldsymbol{L}\times\boldsymbol{L}} & \boldsymbol{0}_{\boldsymbol{L}\times\boldsymbol{L}} & \cdots & \boldsymbol{\Omega}_{\text{Tx},N} \end{bmatrix}_{NL\times NL} \tag{19}$$

Similarly the correlation matrix of GLST Co-MIMO can be denoted as Eq. (18) with $L = 4$.

Fig. 3 has shown the simulation results with GLST Co-MIMO and GLST D-MIMO under the correlated channel conditions. At first we assume the angular spread in each port is equal, for instance $\Delta = 90°$, and we can observe that the symbol error probability of Co-MIMO is very close to that of D-MIMO. However, for more severe correlated conditions ($\Delta = 40°, 20°$), the gap between the two curves is gradually enlarged, e.g. given SNR equal to 20 dB, $\Delta = 40°$, the symbol error rate (SER) of D-MIMO is approaching 0.01, whereas SER of Co-MIMO is about 0.05, the difference is almost five times between each other. However when angular spread decreases to $\Delta = 20°$, nearly ten times margin can be found between each other, where SER of D-MIMO is equal to 0.04 and SER of Co-MIMO is nearly 0.4.

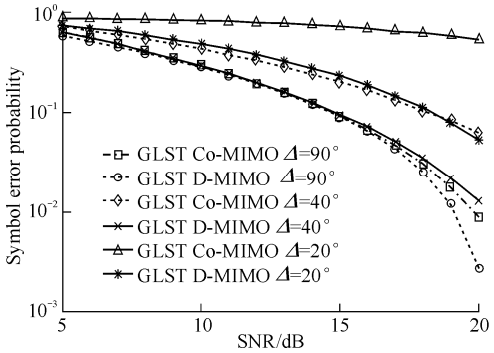

Fig. 3 The comparison between GLST Co-MIMO and GLST D-MIMO according to the symbol error probability criterion

In Fig. 4, we try to simulate the SER performance with unequal angular spread in each port ($\Delta_1 = 90^o, 40^o, 15^o$ and $\Delta_2 = 90^o$). According to the simulation results, we can find that the performance loss of GLST D-MIMO is trivial when Δ_1 changes from 90° to 40°, whereas considerable loss can be found with GLST Co-MIMO. Moreover, we assume one port experience more severe correlated fading conditions with angular spread equal to 15°, in such case GLST D-MIMO still superior to its opponent at $\Delta = 40^o$. Therefore, we can find that GLST D-MIMO has more advantages in combating the correlated fading channels than GLST Co-MIMO in terms of SER performance.

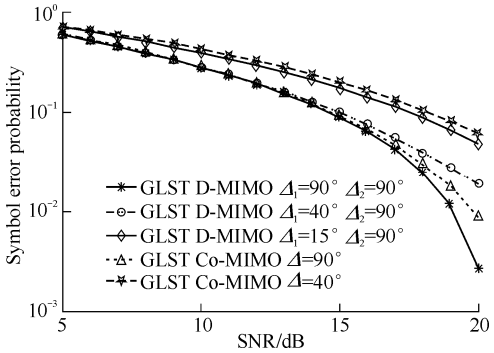

Fig. 4 SER performance with different angular spread in each port

4 Capacity analysis with selection algorithms

In this part we will evaluate the system capacity of GDAS by making use of fast transmit antenna selection algorithms under correlated fading channels. The generalized Shannon bound on capacity has been presented by Foschini and Gans as

$$\boldsymbol{C} = \mathrm{lb}\det\left(\boldsymbol{I} + \frac{\gamma}{K}\boldsymbol{H}_{\mathrm{sel}}^{\mathrm{H}}\boldsymbol{H}_{\mathrm{sel}}\right) \tag{20}$$

where det denotes determinate, $\boldsymbol{I}$ is an $K \times K$ identity matrix (K is the selected transmit antenna numbers), and γ is averaged transmit SNR. Here, $\boldsymbol{H}$ is original $M \times NL$ GDAS channel matrix, $\boldsymbol{H}_{\mathrm{sel}}$ is the selected $M \times NK$ channel matrix, and the corresponding correlated channel matrix can be modeled as in Eq. (3). While, maximizing Eq. (20) is equivalent to maximizing

$$\det\left(\frac{K}{\gamma}\boldsymbol{I} + \boldsymbol{H}_{\mathrm{sel}}^{\mathrm{H}}\boldsymbol{H}_{\mathrm{sel}}\right) \tag{21}$$

At high SNR, we can approximate Eq. (21) by the equation

$$\det\left(\frac{K}{\gamma}\boldsymbol{I} + \boldsymbol{H}_{\mathrm{sel}}^{\mathrm{H}}\boldsymbol{H}_{\mathrm{sel}}\right) \approx \det(\boldsymbol{H}_{\mathrm{sel}}^{\mathrm{H}}\boldsymbol{H}_{\mathrm{sel}}) \tag{22}$$

Here, $\boldsymbol{H}_{\mathrm{sel}}^{\mathrm{H}}\boldsymbol{H}_{\mathrm{sel}}$ is a Hermitian positive definite square matrix, which contains real positive eigen-value, thus by utilizing singular value decomposition, $\det(\boldsymbol{H}_{\mathrm{sel}}^{\mathrm{H}}\boldsymbol{H}_{\mathrm{sel}})$ can be further expressed as

$$\det(\boldsymbol{H}_{\mathrm{sel}}^{\mathrm{H}}\boldsymbol{H}_{\mathrm{sel}}) = \prod_{l}\lambda_l \tag{23}$$

where λ_l is the eigenvalue of $\boldsymbol{H}_{\mathrm{sel}}^{\mathrm{H}}\boldsymbol{H}_{\mathrm{sel}}$. Therefore, to maximize the capacity, the optimal selection is actually the exhaustive search for $\boldsymbol{H}$ with the largest $\prod_l \lambda_l$, but when considering multiuser scenarios, the system load will increase significantly. Thus, a sub optimal method is try to maximize the minimum eigen-value $\lambda_{\min}$ [13], which guarantee the selected channel $\boldsymbol{H}_{\mathrm{sel}}$ with K eigen-value as large as possible. Based on the gerschgorin circle (GC) theorem [12], the distribution of eigen-values can be well approximated.

Theorem 2 The K eigen-values of matrix $\boldsymbol{H}_{\mathrm{sel}} = (h_{i,j})_{M \times NK} \in \mathbf{C}^{M \times NK}$ are included in union set of Gerschgorin circles which centered at $\| \boldsymbol{h}_l \|_2^2$ with radii R_l given by

$$| \lambda_l - \| \boldsymbol{h}_l \|_2^2 | \leqslant \boldsymbol{R}_l = \sum_{k \neq l} | \boldsymbol{h}_k^{\mathrm{H}} \boldsymbol{h}_l | \tag{24}$$

where $\boldsymbol{h}_l$ is the lth column of channel matrix , $\| \boldsymbol{h}_l \|_2^2$ is 2-norm, and $| \boldsymbol{h}_k^{\mathrm{H}} \boldsymbol{h}_l |$ is the inner product between lth and kth column of channel matrix. According to the triangle inequality, the lower bound of $\lambda_{\min}$ can be deduced as

$$\lambda_{\min} \geqslant \min_{l=1,2,\ldots,K}\left(\| \boldsymbol{h}_l \|_2^2 - \sum_{k \neq l} | \boldsymbol{h}_k^{\mathrm{H}} \boldsymbol{h}_l | \right) \tag{25}$$

where a large center of the lth G-circle denote large channel gain of transmit antenna l, and a small radius means low correlation between lth and kth antennas. From which we can obtain an optimal eigen-value from the selected G-set, and update $\boldsymbol{H}_{\mathrm{sel}}$ with largest channel vector $\boldsymbol{h}_l$. Moreover, due to the geographically separated distributed antennas, the system performance is fluctuated considerably with the

different path loss level. Thus, in the aim of fairness, a sub optimal power allocation scheme has been proposed to overcome the effects of large scale fading, where the transmit power is proportional allocated according to the distance from mobile user to each port. Furthermore, in D-MIMO cases, in order to maximize the capacity, we selected the optimal K_p antennas from each port and combined them together to form an optimal correlation matrix, which result in a small channel condition number and maximized the projection height.

In Fig. 5 we assume the antenna spacing is half of the wavelength, SNR is equal to 20 dB, and without loss of any generality, the angle of departure is set to zero degree. When considering the GDAS (M=2, N=1, L=4) Co-MIMO case, we selected K antennas ($K = M$) with larger norm and smaller fading correlations from the GC set (L antennas). According to Fig. 5, the rightmost curve demonstrates the performance of GC antenna selection algorithms with angular spread equals to $90°$, from which nearly ninety percent of system capacity concentrated in the vicinity of $7.8\ \text{bit}\cdot\text{s}^{-1}\cdot\text{Hz}^{-1}$, while there are nearly $1.5\ \text{bit}\cdot\text{s}^{-1}\cdot\text{Hz}^{-1}$ loss as to none-antennal selection case. Moreover, when angular spread decreased to $5°$, GC based algorithms still outperform to its opponent.

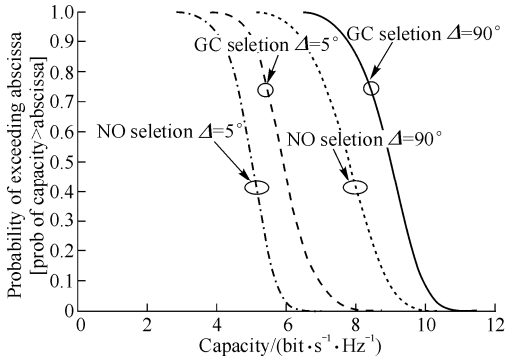

Fig. 5 Capacity ccdf of different PAS with SNR = 20 dB

In Fig. 6, GC antenna selection algorithms have been further considered in GDAS (M=4, N=4, L=4) D-MIMO conditions, where K=4 optimal antennas are selected from the two nearest ports with total antenna number equal to eight (Note: $K_p = 2$ in each port). Here two extreme conditions: AS equals to $90°$ and $5°$, are simulated representing well- and ill- conditioned channels, respectively, and simple power allocation has been employed according to the distance from MT to each port in order to eliminate the effect of large scale fading. Through Monte Carlo simulation, we present simulation results of ergodic capacity performances with the variation of the angular spread, from which D-MIMO with GC algorithms outperform others in all cases. However in ill-conditioned channels, we can find that the loss of system performance is trivial between two D-MIMO cases, but the capacity gap is enlarged between Co-MIMO and D-MIMO with the increase of SNR. This means that D-MIMO with GC antenna selection method is the best choice when compared with Co-MIMO cases under correlated fading conditions.

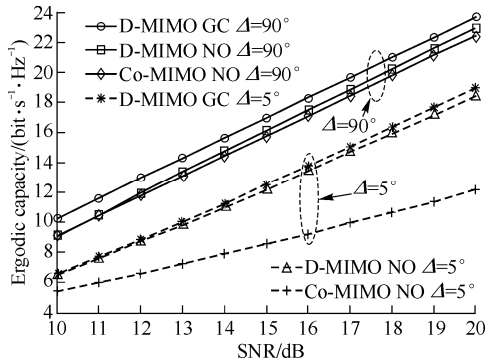

Fig. 6 Ergodic capacity performance of D-MIMO with GC algorithms

5 Conclusions

In this study, the architecture of distributed GLST has been considered in order to achieve the tradeoff between multiplexing gain and diversity gain. In such a way, we have the same spectrum efficiency with VBLAST but without requiring the receive antenna numbers be greater than or at least equal with transmitters. Moreover, we share a common framework in deducing the correlation coefficients according to series of Bessel function. Monte Carlo simulations have revealed that under the given distributed antenna system, GLST D-MIMO outperform GLST Co-MIMO in semi-correlated fading channels. Furthermore, we have utilized fast antenna selection algorithms based on Gerschgorin circles theorem which can improve the system capacity considerably.

Acknowledgements

The work was Supported by the Hi-Tech Research and Development Program of China (2009AA011502), China Important National Science &Technology Specific Projects (2009ZX03007-003-01), and the National Natural Science Foundation of China (60772113).

Appendix

A.1 Proof of Eq. (9)

According to the series representation of Bessel function in

Eq. (5), we can obtain the numerical expression of correlation coefficient $\Omega_{x,x}$ as

$$\Omega_{x,x}=\int_{\theta-\Delta}^{\theta+\Delta}\cos[z\sin\Phi]f(\Phi)\mathrm{d}\Phi=\int_{\theta-\Delta}^{\theta+\Delta}\left[J_0(z)+2\sum_{m=1}^{\infty}J_{2m}(z)\cos(2m\Phi)\right]\cdot\left[N_0\exp\left(\frac{-\sqrt{2}\,|\Phi-\theta|}{\sigma}\right)\left(\sqrt{2}\sigma\right)^{-1}\right]\mathrm{d}\Phi \quad (A.1)$$

where Eq. (A.1) can be simplified by introducing variables a,b and τ, which can be denoted as

$$\left.\begin{aligned}a&=\frac{N_0}{\sqrt{2}\sigma}J_0(z)\\b&=\frac{2N_0}{\sqrt{2}\sigma}\sum_{m=1}^{\infty}J_{2m}(z)\\\tau&=\frac{\sqrt{2}}{\sigma}\end{aligned}\right\} \quad (A.2)$$

Then we can obtain the following equation

$$\Omega_{x,x}=\int_{\theta-\Delta}^{\theta+\Delta}[a+b\cos(2m\Phi)]\mathrm{e}^{-\tau|\Phi-\theta|}\,\mathrm{d}\Phi=\int_{-\Delta}^{+\Delta}[a+b\cos(2m(u+\theta))]\mathrm{e}^{-\tau|u|}\,\mathrm{d}u \quad (A.3)$$

where we substitute u for $\Phi-\theta$ in Eq. (A.3), and then the first part of integration can be expressed as

$$\Omega_{x,x}^{1}=\int_{-\Delta}^{\Delta}a\,\mathrm{e}^{-\tau|u|}\,\mathrm{d}u=2a\int_{0}^{\Delta}\mathrm{e}^{-\tau u}\,\mathrm{d}u=\frac{2a}{\tau}(1-\mathrm{e}^{-\tau\Delta})=\frac{2N_0}{\tau\sqrt{2}\sigma}J_0(z)(1-\mathrm{e}^{-\tau\Delta})=J_0(z) \quad (A.4)$$

$$\Omega_{x,x}^{1}=\int_{-\Delta}^{\Delta}a\,\mathrm{e}^{-\tau|u|}\,\mathrm{d}u=2a\int_{0}^{\Delta}\mathrm{e}^{-\tau u}\,\mathrm{d}u=\frac{2a}{\tau}(1-\mathrm{e}^{-\tau\Delta})=J_0(z)$$

Moreover we set $\xi=2\,\mathrm{m}$, and the second part of integration can be denoted as

$$\Omega_{x,x}^{2}=\int_{-\Delta}^{\Delta}b\cos[\xi(u+\theta)]\mathrm{e}^{-\tau|u|}\,\mathrm{d}u=\int_{0}^{\Delta}2b\cos(\xi\theta)\cos(\xi u)\mathrm{e}^{-\tau u}\,\mathrm{d}u=\frac{2b\cos(\xi\theta)}{\tau^2+\xi^2}\left[\tau+\mathrm{e}^{-\tau\Delta}\left(\xi\sin(\xi\Delta)-\tau\cos(\xi\Delta)\right)\right] \quad (A.5)$$

where we substitute variable b in Eq. (A.5), and then the correlation coefficient $\Omega_{x,x}$ can be rewritten as

$$\Omega_{x,x}=\Omega_{x,x}^{1}+\Omega_{x,x}^{2}=J_0(z)+2\tau N_0\sum_{\xi=2m>0}\frac{J_{\xi}(z)\cos(\xi\theta)}{\xi^2+\tau^2}\cdot\left[\tau+\mathrm{e}^{-\tau\Delta}\left(\xi\sin(\xi\Delta)-\tau\cos(\xi\Delta)\right)\right] \quad (A.6)$$

A.2 Proof of formulation Eq. (10)

Similarly, according to Eq. (5) the cross correlation coefficient $\Omega_{x,y}$ can be derived as

$$\Omega_{x,y}=\int_{\theta-\Delta}^{\theta+\Delta}\sin(z\sin\Phi)f(\Phi)\mathrm{d}\Phi=\int_{\theta-\Delta}^{\theta+\Delta}\left[2\sum_{m=0}^{\infty}J_{2m+1}(z)\sin[(2m+1)\Phi]\right]\cdot\left[N_0\exp\left(\frac{-\sqrt{2}\,|\Phi-\theta|}{\sigma}\right)\left(\sqrt{2}\sigma\right)^{-1}\right]\mathrm{d}\Phi \quad (A.7)$$

where we use symbols c,v and Υ to substitute the corresponding expressions in Eq. (A.7), which can be denoted as

$$\left.\begin{aligned}c&=\frac{2N_0}{\sqrt{2}\sigma}\sum_{m=0}^{\infty}J_{2m+1}(z)\\\tau&=\frac{\sqrt{2}}{\sigma}\\v&=2m+1\end{aligned}\right\} \quad (A.8)$$

where we use $u=\Phi-\theta$ and obtain the following expression

$$\Omega_{x,y}=\int_{\theta-\Delta}^{\theta+\Delta}c\sin(v\Phi)\exp(-\tau\,|\Phi-\theta\,|)\mathrm{d}\Phi=\int_{-\Delta}^{\Delta}c\sin[v(u+\theta)]\mathrm{e}^{-\tau|u|}\,\mathrm{d}\Phi=2c\sin(v\theta)\left\{\frac{\mathrm{e}^{-\Upsilon\Delta}(v\sin(v\Delta)-\tau\cos(v\Delta))+\tau}{v^2+\tau^2}\right\}=2N_0\tau\sum_{\upsilon=2m+1>0}\frac{J_{\upsilon}(z)\sin(\upsilon\theta)}{\upsilon^2+\tau^2}\cdot\left[\tau+\mathrm{e}^{-\tau\Delta}(\upsilon\sin(\upsilon\Delta)-\tau\cos(\upsilon\Delta))\right] \quad (A.9)$$

References

1. Saleh A, Rustako A, Roman R. Distributed antennas for indoor radio communications. IEEE Transactions on Communications, 1987, 35(12): 1245–1251
2. Roh W, Paulraj A. MIMO channel capacity for the distributed antenna. Proceedings of the 56th Vehicular Technology Conference (VTC-Fall'02), Vol 2, Sep 24–28, 2002, Vancouver, Canada. Piscataway NJ, USA: IEEE, 2002: 706–709
3. Tao M X, Cheng R S. Generalized layered space-time codes for high data rate wireless communications. IEEE Transactions on Wireless Communications, 2004, 3(4): 1067–1075
4. Zhang Z F, Zhang H B. Performance evaluation of MIMO technology for LTEAdvanced system. Journal of Chongqing University of Posts and Telecommunications (Natural Science Edition), 2010, 22(2): 140–145 (in Chinese)
5. Lee W. Effects on correlation between two mobile radio base-station antennas. IEEE Transactions on Communications, 1973, 21(11): 1214–1224
6. Gore D A, Paulraj A J. MIMO antenna subset selection with space time coding. IEEE Transactions on Signal Processing, 2002, 50(10): 2580–2588
7. Khan M, Vesilo R, Davis L, et al. User and transmit antenna selection for MIMO broadcast wireless channels with linear receivers. Proceedings of the Australasian Telecommunication Networks and Applications Conference (ATNAC'08), Dec 7–10, 2008, Adelaide, Australia.Piscataway NJ, USA: IEEE, 2008: 276–281
8. Salz J, Winters J H. Effect of fading correlation on adaptive arrays in digital mobile radio. IEEE Transactions on Vehicular Technology, 1994, 43(4): 1049–1057

9. Wolniansky P W, Foschini G J, Golden G D. V-blast: an architecture for realizing very high data rates over the rich-scattering wireless channel. Proceedings of the URSI International Symposium on Signals, Systems and Electronics (ISSSE'98), Sep 29–Oct 2, 1989, Pisa, Italy. Piscataway NJ, USA: IEEE,1998: 295–300
10. Spiegel M R, Lipschutz S, Liu J. Mathematical handbook of formulas and tables. New York, NY, USA: McGraw-Hill, 2008
11. Spatial channel model for MIMO simulations.3GPP TR 25.996 V9.0.0. 2009
12. Horn R A, Johnson C R. Topics in matix analysis. Cambridge, UK: Cambridge University Press, 1991
13. Zhang H Y, Dai H Y. Fast transmit antenna selection algorithms for MIMO systems with fading correlation. Proceedings of the 60th Vehicular Technology Conference (VTC-Fall'04): Vol 3, Sep 26–29, 2004, Los Angeles, CA, USA. Piscataway, NJ, USA: IEEE, 2004: 1638–1642

(Editor: ZHANG Ying)

From p. 15

9. Jitvanichphaibool K, Rui Z, Ying C L. Optimal resource allocation for two-way relay-assisted OFDMA. IEEE Transactions on Vehicular Technology, 2009, 58(7): 3311–3321
10. Chin K H, Rui Z, Ying C L. Two-way relaying over OFDM: optimized tone permutation and power allocation. Proceedings of the IEEE International Conference on Communications (ICC'08), May 19–23, 2008, Beijing, China. Piscataway, NJ, USA: IEEE, 2008: 3908–3912
11. Hammerstrom I, Kuhn M, Esli C, et al. MIMO two-way relaying with transmit CSI at the relay. Proceedings of the 8th Workshop on Signal Processing Advances in Wireless Communications (SPAWC'07), Jun 17–20, 2007, Helsinki, Finland. Piscataway, NJ, USA: IEEE, 2007: 5p
12. Rui Z, Chin C C, Ying C L, et al. On capacity region of two-way multi-antenna relay channel with analogue network coding. Proceedings of the IEEE International Conference on Communications (ICC'09), Jun 14–18, 2009, Dresden, Germany. Piscataway, NJ, USA: IEEE, 2009: 25–30
13. Wen Y W, Renbiao W. Capacity maximization for OFDM two-hop relay system with separate power constraints. IEEE Transactions on Vehicular Technology, 2009, 58(9): 4943–4954
14. Wong C Y, Cheng R S, Letief K B, et al. Multiuser OFDM with adaptive subcarrier, bit, and power allocation. IEEE Journal on Selected Areas in Communications, 1999, 17(10): 1747–1758
15. Boyd S, Vandenberghe L. Convex optimization. London, UK: Cambridge University Press, 2004
16. Zhang Q, Zhang J, Shao C, et al. Power allocation for regenerative relay channel with Rayleigh fading. Proceedings of the 59th Vehicular Technology Conference (VTC-Spring'04): Vol 2, May 17–19, 2004, Milan, Italy. Piscataway, NJ, USA: IEEE, 2004: 1167–1171

(Editor: WANG Xu-ying)